

# Magnetic black holes within Einstein-AdS gravity coupled to nonlinear electrodynamics, extended phase space thermodynamics and Joule–Thomson expansion

S. I. Kruglov <sup>1</sup>

*Department of Physics, University of Toronto,  
60 St. Georges St., Toronto, ON M5S 1A7, Canada  
Canadian Quantum Research Center,  
204-3002 32 Ave Vernon, BC V1T 2L7, Canada*

## Abstract

Einstein’s gravity in AdS space coupled to nonlinear electrodynamics is studied. We analyse the metric, mass functions and corrections to the Reissner–Nordström solution. Magnetic black holes thermodynamics in extended phase space is investigated. We formulate the first law of black hole thermodynamics showing that the generalized Smarr relation holds. The black hole stability is studied by evaluating the Gibbs free energy and heat capacity. To study the cooling and heating phase transitions of black holes we consider the Joule–Thomson isenthalpic expansion. The Joule–Thomson coefficient and the inversion temperature are calculated.

## 1 Introduction

Studying black holes could shed light on quantum gravity which is not developed yet. In the last decades the behavior of black holes is a subject of intensive investigations which was stimulated recently by the Event Horizon Telescope collaboration, detected the shadows of M87\* and Sagittarius A\* black holes [1]. Hawking and Bekenstein showed that black holes are the thermodynamic systems [2, 3, 4] (see also [5, 6, 7]) with the entropy and the temperature connected with black holes surface area and surface gravity, respectively. The four laws of black hole mechanics were determined which are analogous to the ordinary thermodynamics laws [5]. The interest in Anti-de Sitter (AdS) space-time is due to AdS/CFT correspondence (the holographic principle) [8] showing the connection of gravity in AdS space-time with the

---

<sup>1</sup>E-mail: serguei.kruglov@utoronto.ca

conformal field theory (CFT). The holographic principle has applications in condensed matter physics. Hawking and Page discovered that black holes first-order phase transitions take place in AdS space-time with negative cosmological constant [9]. Within AdS/CFT correspondence such phase transitions correspond to a confinement/deconfinement phase transitions [10]. It was shown in [11, 12, 13, 14, 15, 16] that phase transitions in AdS black holes mimic Van der Waals liquid-gas phase transitions. Einstein-AdS black hole thermodynamics in an extended phase space was studied [17, 18, 19, 20], where the cosmological constant is treated as thermodynamic pressure and the black hole mass is interpreted as enthalpy.

Black hole thermodynamics in Einstein-AdS gravity coupled to Born-Infeld electrodynamics, which is a special case of nonlinear electrodynamics (NED), was studied in [21, 22, 23, 24, 25, 26, 27, 28, 29, 30, 31, 32, 33] and in extended phase space in [34, 35, 36, 37, 38]. Black hole thermodynamics in other NED models coupled to Einstein-AdS gravity was investigated in [39, 40, 41, 42, 43]. The Joule-Thomson black hole expansion firstly was studied in [44, 45] and later in [46, 47, 48, 49, 39, 40, 41, 42, 50].

The interest in the model under consideration is in its simplicity. The mass and metric functions are expressed via elementary functions. The studying different models is useful to see different details in its behavior.

The structure of paper is as follows. In Section 2 we find and analyse the metric function possessing asymptotic with corrections to the Reissner-Nordström solution. The first law of black hole thermodynamics in the extended phase space is formulated in Section 3. The thermodynamic magnetic potential and the conjugate to the NED coupling are calculated. It is proven that the generalized Smarr relation holds. In Section 4 we study the stability of black holes. The critical temperature, critical pressure, the Gibbs free energy and heat capacity are calculated. It is shown that phase transitions occur and black hole thermodynamics is similar to Van der Waals thermodynamics. In Section 5 the Joule-Thomson adiabatic expansion is investigated. We calculate the Joule-Thomson coefficient and the inversion temperature. In Section 6 we make a conclusion.

Throughout the paper the units  $c = \hbar = 1$ ,  $k_B = 1$  are used.

## 2 Black hole solution of Einstein-AdS gravity coupled to NED

The action of Einstein-AdS gravity coupled to NED is given by [21]

$$I = \int d^4x \sqrt{-g} \left( \frac{R - 2\Lambda}{16\pi G_N} + \mathcal{L}(\mathcal{F}) \right), \quad (1)$$

where  $G_N$  is the Newton's constant,  $\Lambda = -3/l^2$  being the negative cosmological constant and  $l$  is the AdS radius. We consider the NED Lagrangian in the form [51]

$$\mathcal{L}(\mathcal{F}) = -\frac{\mathcal{F}}{4\pi(1 + (2\beta\mathcal{F})^{3/2})}, \quad (2)$$

with the Lorentz invariant  $\mathcal{F} = F^{\mu\nu}F_{\mu\nu}/4 = (B^2 - E^2)/2$ , and  $E$  and  $B$  are the electric and magnetic fields, correspondingly. At the limit  $\beta \rightarrow 0$  Lagrangian (2) is converted into the Maxwell Lagrangian. The field equations obtained from action (1) are

$$R_{\mu\nu} - \frac{1}{2}g_{\mu\nu}R + \Lambda g_{\mu\nu} = 8\pi G_N T_{\mu\nu}, \quad (3)$$

$$\partial_\mu (\sqrt{-g} \mathcal{L}_{\mathcal{F}} F^{\mu\nu}) = 0, \quad (4)$$

where  $\mathcal{L}_{\mathcal{F}} = \partial\mathcal{L}(\mathcal{F})/\partial\mathcal{F}$ . The energy-momentum tensor is given by

$$T_{\mu\nu} = F_{\mu\rho}F_{\nu}{}^\rho \mathcal{L}_{\mathcal{F}} + g_{\mu\nu} \mathcal{L}(\mathcal{F}). \quad (5)$$

We explore the line element with the spherical symmetry

$$ds^2 = -f(r)dt^2 + \frac{1}{f(r)}dr^2 + r^2(d\theta^2 + \sin^2(\theta)d\phi^2). \quad (6)$$

The black hole is considered here as a magnetic monopole where the magnetic field is  $B = q/r^2$  and  $q$  is the magnetic charge. The metric function found from Eq. (3) is [52]

$$f(r) = 1 - \frac{2m(r)G_N}{r}, \quad (7)$$

where the mass function is defined as

$$m(r) = m_0 + 4\pi \int_0^r \rho(r)r^2 dr, \quad (8)$$

with  $m_0$  being the Schwarzschild mass (an integration constant), and  $\rho$  is the energy density. We obtain from Eq. (5) the magnetic energy density including the AdS space-time energy density

$$\rho = \frac{q^2 r^2}{8\pi(r^6 + \beta^{3/2} q^3)} - \frac{3}{8\pi G_N l^2}. \quad (9)$$

Making use of Eqs. (8) and (9) one finds the mass function

$$\begin{aligned} m(r) = m_0 + \frac{q^{3/2}}{24\sqrt[4]{\beta}} & \left[ \sqrt{3} \ln \frac{r^2 - \sqrt{3}\sqrt[4]{\beta}q^2 r + \sqrt{\beta}q}{r^2 + \sqrt{3}\sqrt[4]{\beta}q^2 r + \sqrt{\beta}q} + 4 \arctan \left( \frac{r}{\sqrt[4]{\beta}q^2} \right) \right. \\ & \left. + 2 \arctan \left( \sqrt{3} + \frac{2r}{\sqrt[4]{\beta}q^2} \right) - 2 \arctan \left( \sqrt{3} - \frac{2r}{\sqrt[4]{\beta}q^2} \right) \right] - \frac{r^3}{2G_N l^2}. \end{aligned} \quad (10)$$

We obtain the magnetic energy (magnetic mass) of the black hole

$$m_M = \frac{q^2}{2} \int_0^\infty \frac{r^4}{r^6 + (\beta q^2)^{3/2}} dr = \frac{\pi q^{3/2}}{6\sqrt[4]{\beta}}, \quad (11)$$

which is finite. As a result, the NED leads to the absence of singularities. By virtue of Eqs. (7) and (10) one finds the metric function

$$\begin{aligned} f(r) &= 1 - \frac{2m_0 G_N}{r} - \frac{q^{3/2} G_N g(r)}{12\sqrt[4]{\beta} r} + \frac{r^2}{l^2}, \\ g(r) &= \sqrt{3} \ln \frac{r^2 - \sqrt{3}\sqrt[4]{\beta}q^2 r + \sqrt{\beta}q}{r^2 + \sqrt{3}\sqrt[4]{\beta}q^2 r + \sqrt{\beta}q} + 4 \arctan \left( \frac{r}{\sqrt[4]{\beta}q^2} \right) \\ &+ 2 \arctan \left( \sqrt{3} + \frac{2r}{\sqrt[4]{\beta}q^2} \right) - 2 \arctan \left( \sqrt{3} - \frac{2r}{\sqrt[4]{\beta}q^2} \right). \end{aligned} \quad (12)$$

In the case when the Schwarzschild mass is zero ( $m_0 = 0$ ) and as  $r \rightarrow 0$ , we obtain

$$f(r) = 1 + \frac{r^2}{l^2} - \frac{G_N r^4}{5q\beta^{3/2}} + \frac{G_N r^{10}}{11q^4\beta^3} + \mathcal{O}(r^{13}). \quad (13)$$

Thus, the black hole is regular ( $f(0) = 1$ ) and the metric function (13) has a de-Sitter core. With the help of Eq. (12), when  $\Lambda = 0$ , and as  $r \rightarrow \infty$  one finds

$$f(r) = 1 - \frac{2MG_N}{r} + \frac{q^2 G_N}{r^2} + \mathcal{O}(r^{-3}). \quad (14)$$

As a result,  $M = m_0 + m_M$  is the ADM mass. Equation (14) shows that black holes possess corrections to the Reissner–Nordström solution. At  $\beta = 0$  the metric (14) is converted into the Reissner–Nordström metric. The metric function (12) plots are given in Fig. 1 at  $m_0 = 0$ ,  $G_N = 1$ ,  $l = 15$ . Figure 1 shows that black holes can have one or two horizons. If coupling  $\beta$  increases the event horizon radius decreases. When magnetic charge  $q$  increases, the event horizon radius also increases.

### 3 First law of black hole thermodynamics and Smarr relation

In extended phase space the positive pressure is given by  $P = -\Lambda/(8\pi)$  [53, 54, 55, 56, 57] and coupling  $\beta$  is a thermodynamic variable which is conjugated to vacuum polarisation. The black hole mass  $M$  is treated as a chemical enthalpy ( $M = U + PV$ ,  $U$  is the internal energy). With the help of the Euler’s dimensional analysis with  $G_N = 1$  [58], [53] we have dimensions as  $[M] = L$ ,  $[S] = L^2$ ,  $[P] = L^{-2}$ ,  $[J] = L^2$ ,  $[q] = L$ ,  $[\beta] = L^2$  and

$$M = 2S \frac{\partial M}{\partial S} - 2P \frac{\partial M}{\partial P} + 2J \frac{\partial M}{\partial J} + q \frac{\partial M}{\partial q} + 2\beta \frac{\partial M}{\partial \beta}. \quad (15)$$

The vacuum polarization is  $\mathcal{B} = \partial M / \partial \beta$  [20]. For non-rotating black holes one has  $J = 0$ ; the black hole entropy  $S$ , volume  $V$  and pressure  $P$  are given by

$$S = \pi r_+^2, \quad V = \frac{4}{3} \pi r_+^3, \quad P = -\frac{\Lambda}{8\pi} = \frac{3}{8\pi l^2}. \quad (16)$$

From Eq. (12) we find the black hole mass that is understood as a chemical enthalpy

$$M(r_+) = \frac{r_+}{2G_N} + \frac{r_+^3}{2G_N l^2} + \frac{\pi q^{3/2}}{6\sqrt[4]{\beta}} - \frac{q^{3/2} g(r_+)}{24\sqrt[4]{\beta}}, \quad (17)$$

with  $r_+$  being the event horizon radius,  $f(r_+) = 0$ . Making use of Eq. (17) one obtains the vacuum polarization  $B$  and the thermodynamic potential  $\Phi$

$$B = \frac{\partial M(r_+)}{\partial \beta} = \frac{q^{3/2} g(r_+)}{96\beta^{5/4}} - \frac{\pi q^{3/2}}{24\beta^{5/4}} + \frac{q^2 r_+^5}{8\beta(r_+^6 + (q\sqrt{\beta})^3)},$$

$$\Phi = \frac{\partial M(r_+)}{\partial q} = \frac{\pi\sqrt{q}}{4\sqrt[4]{\beta}} - \frac{\sqrt{q} g(r_+)}{16\sqrt[4]{\beta}} + \frac{q r_+^5}{4(r_+^6 + (q\sqrt{\beta})^3)}. \quad (18)$$

The Hawking temperature is defined as

$$T = \frac{f'(r)|_{r=r_+}}{4\pi}, \quad (19)$$

where  $f'(r) = \partial f(r)/\partial r$ . By virtue of Eq. (17) we obtain

$$\frac{\partial M(r_+)}{\partial r_+} = \frac{1}{2} + \frac{3r_+^2}{2l^2} - \frac{q^2 r_+^4}{2(r_+^6 + (q\sqrt{\beta})^3)}. \quad (20)$$

From Eqs. (12), (19) and (20), one finds the Hawking temperature

$$T = \frac{1}{4\pi} \left( \frac{1}{r_+} + \frac{3r_+}{l^2} - \frac{q^2 r_+^3}{r_+^6 + (q\sqrt{\beta})^3} \right). \quad (21)$$

As  $\beta \rightarrow 0$  Eq. (21) becomes the Hawking temperature of Maxwell-AdS black hole. With the aid of Eqs. (16), (18) and (21) we obtain the first law of black hole thermodynamics

$$dM = TdS + VdP + \Phi dq + \mathcal{B}d\beta. \quad (22)$$

Equation (22) represents the modification of ordinary the first law of thermodynamics by the additional term  $\mathcal{B}d\beta$ . The plots of  $\Phi$  and  $\mathcal{B}$  versus  $r_+$  are given in Fig. 2. In accordance with Fig. 2 (left panel) when parameter  $\beta$  increases the magnetic potential  $\Phi$  decreases. When  $r_+ \rightarrow \infty$  the magnetic potential vanishes ( $\Phi(\infty) = 0$ ), and at  $r_+ = 0$  potential  $\Phi$  is finite. Making use of Eq. (18) one finds  $\Phi(0) = \pi\sqrt{q}/(4\sqrt[4]{\beta})$  ( $g(0) = 0$ ). According to Fig. 2 there is a maxima of the functions  $\Phi(r_+)$ . When  $\beta \rightarrow 0$  we have  $\Phi \rightarrow q/(4r_+)$ . Figure 2 (right panel) shows that when  $r_+ = 0$  the vacuum polarization is finite and as  $r_+ \rightarrow \infty$ , vacuum polarisation  $\mathcal{B}$  vanishes ( $\mathcal{B}(\infty) = 0$ ).

From Eqs. (15), (16), (17) and (22) we obtain the generalized Smarr relation

$$M = 2ST - 2PV + q\Phi + 2\beta\mathcal{B}. \quad (23)$$

## 4 Thermodynamics of black holes and phase transitions

Making use of Eq. (21) we obtain the black hole equation of state (EoS)

$$P = \frac{T}{2r_+} - \frac{1}{8\pi r_+^2} + \frac{q^2 r_+^2}{8\pi(r_+^6 + (q\sqrt{\beta})^3)}. \quad (24)$$

As  $\beta \rightarrow 0$  Eq. (24) becomes EoS of charged Maxwell-AdS black hole [56]. Equation (24) mimics the Van der Waals EoS if the specific volume is treated as  $v = 2l_P r_+$  ( $l_P = \sqrt{G_N} = 1$ ) [56]. Then Eq. (24) becomes

$$P = \frac{T}{v} - \frac{1}{2\pi v^2} + \frac{2q^2 v^2}{\pi(v^6 + 64(q\sqrt{\beta})^3)}. \quad (25)$$

Critical points (inflection points) of the  $P - v$  diagrams obey equations as follows:

$$\begin{aligned} \frac{\partial P}{\partial v} &= -\frac{T}{v^2} + \frac{1}{\pi v^3} + \frac{8q^2 v(32(q\sqrt{\beta})^3 - v^6)}{\pi(v^6 + 64(q\sqrt{\beta})^3)^2} = 0, \\ \frac{\partial^2 P}{\partial v^2} &= \frac{2T}{v^3} - \frac{3}{\pi v^4} + \frac{8q^2(5v^{12} - 800(q\sqrt{\beta})^3 v^6 + 2048(q\sqrt{\beta})^6)}{\pi(v^6 + 64(q\sqrt{\beta})^3)^3} = 0. \end{aligned} \quad (26)$$

With the help of Eq. (26) we obtain the equation for critical points  $v_c$

$$(v_c^6 + 64(q\sqrt{\beta})^3)^3 - 8q^2 v_c^4 (3v_c^{12} - 864(q\sqrt{\beta})^3 v_c^6 + 6144(q\sqrt{\beta})^6) = 0. \quad (27)$$

The critical temperature and pressure follow from Eqs. (25) and (26)

$$T_c = \frac{1}{\pi v_c} + \frac{8q^2 v_c^3 (32(q\sqrt{\beta})^3 - v_c^6)}{\pi(v_c^6 + 64(q\sqrt{\beta})^3)^2}, \quad (28)$$

$$P_c = \frac{1}{2\pi v_c^2} + \frac{6q^2 v_c^2 (64(q\sqrt{\beta})^3 - v_c^6)}{\pi(v_c^6 + 64(q\sqrt{\beta})^3)^2}. \quad (29)$$

There are two real solutions  $v_c$  to Eq. (27) for each couplings  $\beta$ . In Table 1 we present only solutions for each  $\beta$  that provide positive values of critical temperatures  $T_c$  and pressures  $P_c$ . The  $P - v$  diagrams are depicted in Fig.

Table 1: Critical values of the specific volume at  $q = 1$

$\beta$	0.1	0.2	0.3	0.4	0.5	0.6	0.7	0.8	0.9	1
$v_c$	4.896	4.891	4.885	4.877	4.868	4.857	4.846	4.833	4.819	4.804

3. At  $q = 1$ ,  $\beta = 0.2$  the critical specific volume is  $v_c \approx 4.891$  and the critical temperature is  $T_c \approx 0.0433$  ( $P_c \approx 0.0033$ ). According to Fig. 3 the pressure vanishes at some points. When the specific volume increases (for small  $v$ ) the pressure increases and the pressure possesses a maximum. After, the pressure

decreases which is similar to the ideal gas. As  $v \rightarrow 0$  the pressure  $P \rightarrow -\infty$ . This behavior is different from the Van der Waals liquid behavior at small  $v$  (or  $r$ ) where as  $v \rightarrow 0$  the pressure  $P \rightarrow \infty$ . The coupling  $\beta$  smoothing the singularity in third term (in right site) of Eq. (25) which becomes zero as  $v \rightarrow 0$  and the dominant term is  $-1/(2\pi v^2)$  which tends to  $-\infty$ . But at  $\beta = 0$  the dominant term is  $2q^2/(\pi v^4)$  which goes to  $+\infty$  as  $v \rightarrow 0$  that is realised in Van der Waals liquid. By virtue of Eqs. (27), (28) and (29) for small  $\beta$ , we obtain

$$v_c^2 = 24q^2 + \mathcal{O}(\beta), \quad T_c = \frac{1}{3\sqrt{6}\pi q} + \mathcal{O}(\beta), \quad P_c = \frac{1}{96\pi q^2} + \mathcal{O}(\beta). \quad (30)$$

Equation (30) shows that at  $\beta = 0$  one obtains the critical points of charged AdS black hole [34]. The critical ratio becomes

$$\rho_c = \frac{P_c v_c}{T_c} = \frac{3}{8} + \mathcal{O}(\beta). \quad (31)$$

The value  $\rho_c = 3/8$  corresponds to the Van der Waals fluid.

Because  $M$  is understood as a chemical enthalpy, the Gibbs free energy (for fixed charge  $q$ , coupling  $\beta$  and pressure  $P$ ) is defined as

$$G = M - TS. \quad (32)$$

From Eqs. (16), (17), (20) and (32) we find

$$G = \frac{r_+}{4} - \frac{2\pi r_+^3 P}{3} + \frac{\pi q^{3/2}}{6\beta^{1/4}} + \frac{q^2 r_+^5}{4(r_+^6 + (q\sqrt{\beta})^3)} - \frac{q^{3/2} g(r_+)}{24\beta^{1/4}}. \quad (33)$$

The plot of the Gibbs free energy  $G$  versus  $T$  for  $\beta = 0.2$  and  $v_c \approx 4.891$ ,  $T_c \approx 0.0433$  is given in Fig. 4. We used Eq. (24) showing that  $P$  and  $T$  are the functions of  $r_+$ . In accordance with subplots 1 and 2 in Fig. 4, at  $P < P_c$  first-order phase transitions occur with the 'swallowtail' behaviour. Subplot 3 shows the second-order phase transition for  $P = P_c$ . According to subplot 4, at the case  $P > P_c$  phase transitions are absent.

The entropy  $S$  versus temperature  $T$  at  $q = 1$ ,  $\beta = 0.2$  is depicted in Fig. 5. Subplots 1 and 2 in Fig. 5 show ambiguous functions of entropy that show first-order phase transitions. According to subplot 3 the second-order phase transition takes place. Low and high entropy states are separated by the critical point. Subplot 4 shows that there are not second-order phase transitions at  $q = 1$ ,  $\beta = 0.2$ ,  $P = 0.005$ .



## 4.1 Heat capacity

To study the black hole local stability we consider the heat capacity which is given by

$$C_q = T \left( \frac{\partial S}{\partial T} \right)_q = \frac{T \partial S / \partial r_+}{\partial T / \partial r_+} = \frac{2\pi r_+ T}{G_N \partial T / \partial r_+}. \quad (34)$$

When the Hawking temperature has an extremum the heat capacity diverges and black hole phase transition occurs. The plot of the Hawking temperature is depicted in Fig. 6 for various parameters  $\beta = 0.1, 0.3, 1$  ( $l = q = 1$ ). According to Fig. 6, the Hawking temperature possesses minima, and therefore, the heat capacity has singularities. The plots of the heat capacity (34) at  $q = l = 1, \beta = 0.1$  ( $G_N = 1$ ) is given in Fig. 7. Figure 7 shows that indeed the heat capacity diverges at the point where the Hawking temperature has a minimum. In this point the phase transition occurs. In the region where the heat capacity is positive the black hole is locally stable, otherwise the black hole is unstable. The heat capacity possesses a singularity at  $\partial T / \partial r_+ = 0$ . Making use of Eq. (21) we find

$$\frac{\partial T}{\partial r_+} = \frac{1}{4\pi} \left( -\frac{1}{r_+^2} + \frac{3}{l^2} - \frac{3q^2 r_+^3 ((q\sqrt{\beta})^3 - r_+^6)}{(r_+^6 + (q\sqrt{\beta})^3)^2} \right).$$

For the case  $l = q = 1, \beta = 0.1$  the approximate real and positive solution to equation  $\partial T / \partial r_+ = 0$  is  $r_s \approx 0.565$ . At this point the black hole undergoes the phase transition from small black hole to large black hole. According to Fig. 7 at  $r_+ > r_s$  the black hole is stable but at  $r_s > r_+ > 0$  the black hole is unstable. Thus, the small sized black holes are unstable and large sized black holes are stable. One can verify that at any parameters we have  $\lim_{r_+ \rightarrow 0} C_q = 0$ , i.e. the heat capacity vanishes at  $r_+ \rightarrow 0$ . But at the infinitesimal radius quantum effects are important [59, 60, 61, 62, 63, 64]. Therefore, without quantum corrections at small radius the stability analyses is not completed. Quantum gravity effects start at the Planck length  $l_P = \sqrt{G_N \hbar / c^3} \approx 1.6 \times 10^{-35}$  m because of quantum fluctuations. It is worth mentioning that the smooth metric fields  $g_{\mu\nu}$  of the classical gravity can not be used at  $r \leq l_P$  but the idea of "space-time foam" [65] is fruitful for describing space-time microscopic degrees of freedom.

## 5 The Joule–Thomson expansion and cooling-heating phase transitions.

The Joule–Thomson expansion takes place when the enthalpy, which is the black hole mass, is constant. This isenthalpic expansion is described by the Joule–Thomson coefficient

$$\mu_J = \left( \frac{\partial T}{\partial P} \right)_M = \frac{1}{C_P} \left[ T \left( \frac{\partial V}{\partial T} \right)_P - V \right] = \frac{(\partial T / \partial r_+)_M}{(\partial P / \partial r_+)_M}, \quad (35)$$

showing the cooling-heating phases. The heating phase takes place when  $\mu_J < 0$ , and the cooling phase occurs if  $\mu_J > 0$ . The Joule–Thomson coefficient represents the slope of the  $P - T$  function. The sign of  $\mu_J$  is changed at the inversion temperature  $T_i$ . The inversion temperature  $T_i$  is defined by equation  $\mu_J(T_i) = 0$ . When the initial temperature is higher than inversion temperature  $T_i$  the cooling phase ( $\mu_J > 0$ ) occurs, and as a result, the final temperature decreases. In the case when the initial temperature is lower than  $T_i$ , the final temperature increases corresponding to the heating phase ( $\mu_J < 0$ ). By taking Eq. (35) and equation  $\mu_J(T_i) = 0$ , one obtains

$$T_i = V \left( \frac{\partial T}{\partial V} \right)_P = \frac{r_+}{3} \left( \frac{\partial T}{\partial r_+} \right)_P. \quad (36)$$

Cooling and heating processes are separated by the inversion temperature. The line of inversion temperature crosses  $P - T$  diagrams maxima [46, 47]. Equation (24) can be written as EoS

$$T = \frac{1}{4\pi r_+} + 2Pr_+ - \frac{q^2 r_+^3}{4\pi(r_+^6 + (q\sqrt{\beta})^3)}. \quad (37)$$

When  $\beta = 0$  Eq. (37) becomes EoS of Maxwell-AdS black holes. Making use of Eq. (17) and equation  $P = 3/(8\pi l^2)$  we obtain

$$P = \frac{3}{4\pi r_+^3} \left[ M(r_+) - \frac{r_+}{2} - \frac{\pi q^{3/2}}{6\beta^{1/4}} + \frac{q^{3/2} g(r_+)}{24\beta^{1/4}} \right]. \quad (38)$$

The  $P - T$  isenthalpic diagrams are depicted in Fig. 8 by using Eqs. (37) and (38). The inversion  $P_i - T_i$  diagram crosses maxima of isenthalpic curves in Fig. 8. With the help of Eqs. (24), (36) and (37) one finds the inversion

pressure  $P_i$

$$P_i = \frac{3q^2 r_+^8}{8\pi (r_+^6 + (\beta q^2)^3)^2} - \frac{1}{4\pi r_+^2}. \quad (39)$$

From Eqs. (37) and (39) one finds the inversion temperature

$$T_i = \frac{q^2 r_+^3 (2r_+^6 - (q\sqrt{\beta})^3)}{4\pi (r_+^6 + (q\sqrt{\beta})^3)^2} - \frac{1}{4\pi r_+}. \quad (40)$$

Putting  $P_i = 0$  in Eq. (39), we obtain the equation for the minimum of the event horizon radius  $r_{min}$

$$2(r_{min}^6 + (\sqrt{\beta}q)^3)^2 - 3q^2 r_{min}^{10} = 0. \quad (41)$$

Making use of Eqs. (40) and (41) at  $\beta = 0$ , one comes to the minimum of the inversion temperature in accordance with Maxwell-AdS magnetic black holes

$$T_i^{min} = \frac{1}{6\sqrt{6}\pi q}, \quad r_{min} = \frac{\sqrt{6}q}{2}. \quad (42)$$

From Eqs. (30) and (42) at  $\beta = 0$  we obtain the relation  $T_i^{min} = T_c/2$  corresponding to Maxwell-AdS black holes [44]. By virtue of Eqs. (39) and (40)  $P_i - T_i$  diagrams are plotted in Fig. 8. Figure 8 shows that the inversion point increases when the black hole mass increases. The inversion diagrams  $P_i - T_i$  are given in Figs. 9 and 10. In accordance with Fig. 9 when magnetic charge  $q$  increases, the inversion temperature also increases. According to Fig. 10 when the coupling  $\beta$  increases the inversion temperature decreases. Making use of Eqs. (35), (37) and (39) we obtain

$$\begin{aligned} \left(\frac{\partial T}{\partial r_+}\right)_M &= -\frac{1}{4\pi r_+^2} + 2P|_M + 2r_+ \left(\frac{\partial P}{\partial r_+}\right)_M - \frac{3q^2 r_+^2 ((q\sqrt{\beta})^3 - r_+^6)}{4\pi (r_+^6 + (q\sqrt{\beta})^3)^2}, \\ \left(\frac{\partial P}{\partial r_+}\right)_M &= \frac{3}{4\pi r_+^4} \left[ \frac{q^{3/2}\pi}{2\beta^{1/4}} - 3M + r_+ - \frac{q^{3/2}g(r_+)}{8\beta^{1/4}} + \frac{q^2 r_+^5}{2(r_+^6 + (q\sqrt{\beta})^3)} \right], \end{aligned} \quad (43)$$

where  $P|_M$  is given in Eq. (38). From Eqs. (35) and (43) one can find the Joule-Thomson coefficient which is the function of the magnetic charge  $q$ , coupling  $\beta$ , black hole mass  $M$  and event horizon radius  $r_+$ . In the case when the Joule-Thomson coefficient is positive,  $\mu_J > 0$ , a cooling process takes place but when  $\mu_J < 0$  a heating process occurs.

## 6 Conclusion

New magnetic black hole solution in Einstein-AdS gravity coupled to NED has been obtained. We have found the metric, mass functions and showed that the magnetic mass of the black hole is finite. It was demonstrated that there are corrections to the Reissner–Nordström solution (at  $\Lambda = 0$ ) due to NED parameter  $\beta$ . The total mass  $M$  which is the sum of the Schwarzschild mass  $m_0$  and magnetic mass  $m_M$  can be considered as ADM mass. We have found the asymptotic as  $r \rightarrow 0$  (at  $m_0 = 0$ ) with a de-Sitter core. Coupling  $\beta$  smoothing singularity so that the black hole is regular. The plots of the metric function  $f(r)$  shown that when coupling  $\beta$  increases at constant magnetic charge the event horizon radius decreases and when magnetic charge increases at constant coupling  $\beta$  the event horizon radius increases. We have formulated the first law of black hole thermodynamics in an extended phase space where positive thermodynamic pressure is connected with negative cosmological constant and dimensional coupling  $\beta$  conjugates the vacuum polarisation. The thermodynamic potential and vacuum polarisation as functions of the event horizon radius have been found and we showed that the generalized Smarr relation holds. We have studied the black holes thermodynamics and phase transitions where the mass of the black hole is treated as the chemical enthalpy. Equation of state has shown that black hole thermodynamics is similar to the Van der Waals liquid–gas thermodynamics. Critical points (inflection points) of the  $P - v$  diagrams have been evaluated corresponding to second-order phase transitions. We have demonstrated that the critical ratio  $\rho_c$  depends in the coupling  $\beta$  and it is different from the Van der Waals value  $3/8$ . The Gibbs free energy has been analysed showing the first-order phase transitions with the ‘swallowtail’ behaviour and second-order phase transitions at critical points. The plots of the entropy  $S$  versus temperature  $T$  for various parameters have been depicted which is the ambiguous function corresponding to first-order phase transitions. The heat capacity is calculated which possesses singularities. When the heat capacity is positive black holes are stable, otherwise they are unstable. We have studied the black hole Joule–Thomson isenthalpic expansions to analyse cooling-heating phase transitions. The JouleThomson coefficient and the inversion temperature separating cooling and heating processes of black holes have been found. The heating phase corresponds to  $\mu_J < 0$ , and the cooling phase takes place at  $\mu_J > 0$ . It was demonstrated that when the black hole mass increases the inversion point increases.

Competing interests: The authors declare there are no competing interests.

This manuscript does not report data.

## References

- [1] Event Horizon Telescope collaboration, K. Akiyama et al., *Astrophys. J.* **875** (2019) L1; *ibid* L2; *ibid* L3; *ibid* L4; *ibid* L5; *ibid* L6.
- [2] S. W. Hawking, Particle Creation by Black Holes, *Commun. Math. Phys.* **43**, 199-220 (1975); Erratum, *ibid* **46**, 206 (1976).
- [3] J. D. Bekenstein, Black holes and the second law, *Lett. Nuovo Cim.* **4**, 737 (1972).
- [4] J. D. Bekenstein, Black holes and entropy, *Phys. Rev. D* **7**, 2333-2346 (1973).
- [5] J. M. Bardeen, B. Carter and S. W. Hawking, The Four laws of black hole mechanics, *Commun. Math. Phys.* **31** (1973), 161-170.
- [6] T. Jacobson, Thermodynamics of space-time: The Einstein equation of state, *Phys. Rev. Lett.* **75** (1995), 1260-1263, [arXiv:gr-qc/9504004].
- [7] T. Padmanabhan, Thermodynamical Aspects of Gravity: New insights, *Rept. Prog. Phys.* **73** (2010), 046901, [arXiv:0911.5004].
- [8] J. M. Maldacena, The Large N limit of superconformal field theories and supergravity, *Int. J. Theor. Phys.* **38** (1999), 1113-1133 (*Adv. Theor. Math. Phys.* **2**, 231 (1998)), [arXiv:hep-th/9711200].
- [9] S. W. Hawking and D. N. Page, Thermodynamics of Black Holes in anti-De Sitter Space, *Commun. Math. Phys.* **87** (1983), 577.
- [10] E. Witten, Anti-de Sitter space, thermal phase transition, and confinement in gauge theories, *Adv. Theor. Math. Phys.* **2**, 505 (1998), [arXiv:hep-th/9803131].

- [11] A. Chamblin, R. Emparan, C. V. Johnson and R. C. Myers, Charged AdS black holes and catastrophic holography, *Phys. Rev. D* **60**, 064018 (1999), [arXiv:hep-th/9902170].
- [12] A. Chamblin, R. Emparan, C. V. Johnson and R. C. Myers, Holography, thermodynamics and fluctuations of charged AdS black holes, *Phys. Rev. D* **60**, 104026 (1999), [arXiv:hep-th/9904197].
- [13] Aruna Rajagopal, David Kubiznak, Robert B. Mann, Van der Waals black hole, *Phys. Lett. B* **737** (2014), 277, [arXiv:1408.1105].
- [14] Terence Delsate, Robert Mann, Van Der Waals Black Holes in d dimensions, *JHEP* **02** (2015), 070, [arXiv:1411.7850].
- [15] Sudhaker Upadhyay, Behnam Pourhassan, Logarithmic corrected Van der Waals black holes in higher dimensional AdS space, *Prog. Theor. Exp. Phys.* **2019** (2019), 013B03, [arXiv:1711.04254].
- [16] Zhen-Ming Xu, Bin Wu, Wen-Li Yang, Van der Waals fluid and charged AdS black hole in the Landau theory, *Class. Quantum Grav.* **38** (2021), 205008, [arXiv:2101.09456].
- [17] B. P. Dolan, Black holes and Boyle’s law? The thermodynamics of the cosmological constant, *Mod. Phys. Lett. A* **30** (2015), 1540002, [arXiv:1408.4023].
- [18] D. Kubiznak and R. B. Mann, Black hole chemistry, *Can. J. Phys.* **93** (2015), 999-1002, [arXiv:1404.2126].
- [19] R. B. Mann, The Chemistry of Black Holes, *Springer Proc. Phys.* **170** (2016), 197-205.
- [20] D. Kubiznak, R. B. Mann, M. Teo, Black hole chemistry: thermodynamics with Lambda, *Class. Quant. Grav.* **34** (2017), 063001, [arXiv:1608.06147].
- [21] S. Fernando and D. Krug, Charged black hole solutions in Einstein–Born–Infeld gravity with a cosmological constant, *Gen. Rel. Grav.* **35** (2003), 129–137, [arXiv:hep-th/0306120].
- [22] T. K. Dey, Born–Infeld black holes in the presence of a cosmological constant, *Phys. Lett. B* **595** (2004), 484–490, [arXiv:hep-th/0406169].

- [23] R.-G. Cai, D.-W. Pang and A. Wang, Born–Infeld black holes in (A)dS spaces, *Phys. Rev. D* **70** (2004), 124034, [arXiv:hep-th/0410158].
- [24] S. Fernando, Thermodynamics of Born–Infeld-anti-de Sitter black holes in the grand canonical ensemble, *Phys. Rev. D* **74** (2006), 104032, [arXiv:hep-th/0608040].
- [25] Y. S. Myung, Y.-W. Kim and Y.-J. Park, Thermodynamics and phase transitions in the Born–Infeld-anti-de Sitter black holes, *Phys. Rev. D* **78** (2008), 084002, [arXiv:arXiv:0805.0187].
- [26] R. Banerjee and D. Roychowdhury, Critical phenomena in Born-Infeld AdS black holes, *Phys. Rev. D* **85** (2012), 044040, [arXiv:arXiv:1111.0147].
- [27] O. Miskovic and R. Olea, Thermodynamics of Einstein–Born–Infeld black holes with negative cosmological constant, *Phys. Rev. D* **77** (2008), 124048, [arXiv:arXiv:0802.2081].
- [28] Wissam A. Chemissany, Mees de Roo, Sudhakar Panda, Thermodynamics of Born–Infeld Black Holes, *Class. Quant. Grav.* **25** (2008), 225009.
- [29] Leonardo Balart, Sharmanthie Fernando, Thermodynamics and Heat Engines of Black Holes with Born–Infeld-type Electrodynamics, *Mod. Phys. Lett. A* **36** (2021), 2150102.
- [30] Kun Meng, Lianzhen Cao, Jiaqiang Zhao, Fuyong Qin, Tao Zhou, Meihua Deng, Dyonic Born–Infeld black hole in four-dimensional Horndeski gravity, *Phys. Lett. B* **819** (2021), 136420.
- [31] F. T. Falciano, M. L. Peñafiel, J. C. Fabris, Entropy bound in Einstein–Born–Infeld black holes, *Phys. Rev. D* **103** (2021), 084046.
- [32] Behnam Pourhassan, M. Dehghani, Mir Faizal, Sanjib Dey, ”-Non- Perturbative Quantum Corrections to a Born-Infeld Black Hole and its Information Geometry”, *Class. Quantum Grav.* **38** (2021), 105001.
- [33] B. Pourhassan, M. Dehghani, S. Upadhyay, Izzet Sakalli, D. V. Singh, Exponential corrected thermodynamics of quantum Born–Infeld BTZ black holes in massive gravity, *Modern Physics Letters A* **37** (2022), 2250230.

- [34] S. Gunasekaran, R. B. Mann and D. Kubiznak, Extended phase space thermodynamics for charged and rotating black holes and Born—Infeld vacuum polarization, *JHEP* **1211** (2012), 110, [arXiv:1208.6251].
- [35] D.-C. Zou, S.-J. Zhang and B. Wang, Critical behavior of Born-Infeld AdS black holes in the extended phase space thermodynamics, *Phys. Rev. D* **89** (2014), 044002, [arXiv:1311.7299].
- [36] S. H. Hendi and M. H. Vahidinia, Extended phase space thermodynamics and P-V criticality of black holes with a nonlinear source, *Phys. Rev. D* **88** (2013), 084045, [arXiv:1212.6128].
- [37] S. H. Hendi, S. Panahiyan and B. Eslam Panah, P-V criticality and geometrical thermodynamics of black holes with Born-Infeld type non-linear electrodynamics, *Int. J. Mod. Phys. D* **25** (2015), 1650010, [arXiv:1410.0352].
- [38] X.-X. Zeng, X.-M. Liu and L.-F. Li, Phase structure of the Born–Infeld-anti-de Sitter black holes probed by non-local observables, *Eur. Phys. J. C* **76** (2016), 616, [arXiv:1601.01160].
- [39] S. I. Kruglov, NED-AdS black holes, extended phase space thermodynamics and Joule—Thomson expansion, *Nucl. Phys. B* **984** (2022), 115949, [arXiv:2209.10524].
- [40] S. I. Kruglov, Magnetic black holes in AdS space with nonlinear electrodynamics, extended phase space thermodynamics and Joule—Thomson expansion, *Int. J. Geom. Meth. Mod. Phys.* **20** (2023), 2350008, [arXiv:2210.10627].
- [41] Sergey Il'ich Kruglov, AdS Black Holes in the Framework of Nonlinear Electrodynamics, Thermodynamics, and Joule—Thomson Expansion, *Symmetry* **14** (2022), 1597, [arXiv:2209.05394].
- [42] S. I. Kruglov, Nonlinearly charged AdS black holes, extended phase space thermodynamics and Joule—Thomson expansion, *Ann. Phys.* **441** (2022) 168894, [arXiv:2208.13662].
- [43] S.I. Kruglov, Rational non-linear electrodynamics of AdS black holes and extended phase space thermodynamics, *Eur. Phys. J. C* **82** (2022), 292, [arXiv:2210.06344].



- [44] Ö. Ökcü and E. Aydiner, Joule–Thomson expansion of the charged AdS black holes, *Eur. Phys. J. C* **77** (2017), 24, [arXiv:1611.06327].
- [45] Ö. Ökcü and E. Aydiner, Joule–Thomson expansion of Kerr–AdS black holes, *Eur. Phys. J. C* **78** (2018), 123.
- [46] H. Ghaffarnejad, E. Yaraie and M. Farsam, Quintessence Reissner–Nordstrom anti de Sitter black holes and Joule–Thomson effect, *Int. J. Theor. Phys.* **57** (2018), 1671, [arXiv:1802.08749].
- [47] C. L. A. Rizwan, A. N. Kumara, D. Vaid and K. M. Ajith, Joule–Thomson expansion in AdS black hole with a global monopole, *Int. J. Mod. Phys. A* **33** (2018), 1850210, [arXiv:1805.11053].
- [48] M. Chabab, H. El Moumni, S. Iraoui, K. Masmar and S. Zhizeh, Joule–Thomson Expansion of RN-AdS Black Holes in  $f(R)$  gravity, *Lett. High Energy Phys.* **05** (2018), 02, [arXiv:1804.10042].
- [49] B. Mirza, F. Naeimipour and M. Tavakoli, Joule–Thomson expansion of the quasitopological black holes, *Frontiers in Physics* **9** (2021), 628727, [arXiv:2105.05047].
- [50] S. I. Kruglov, Magnetically Charged AdS Black Holes and Joule–Thomson Expansion, *Grav. Cosm.* **28**, (2023) 57.
- [51] S. I. Kruglov, Nonlinear Electrodynamics and Magnetic Black Holes, *Annalen Phys. (Berlin)* **529** (2017), 1700073 [arXiv:1708.07006].
- [52] K. A. Bronnikov, Regular magnetic black holes and monopoles from nonlinear electrodynamics, *Phys. Rev. D* **63** (2001), 044005, [arXiv:gr-qc/0006014].
- [53] D. Kastor, S. Ray and J. Traschen, Enthalpy and the Mechanics of AdS Black Holes, *Class. Quant. Grav.* **26** (2009), 195011, [arXiv:0904.2765].
- [54] B. P. Dolan, The cosmological constant and the black hole equation of state, *Class. Quant. Grav.* **28** (2011), 125020, [arXiv:1008.5023].
- [55] M. Cvetič, G. W. Gibbons, D. Kubiznak and C. N. Pope, Black Hole Enthalpy and an Entropy Inequality for the Thermodynamic Volume, *Phys. Rev. D* **84** (2011), 024037, [arXiv:1012.2888].

- [56] D. Kubiznak, R. B. Mann, P-V criticality of charged AdS black holes, *JHEP* **07** (2012), 033, [arXiv:1205.0559].
- [57] Wan Cong, D. Kubiznak, R. B. Mann and M. Visser, Holographic CFT Phase Transitions and Criticality for Charged AdS Black Holes, *JHEP* **08** (2022), 174, [arXiv:2112.14848].
- [58] L. Smarr, Mass formula for Kerr black holes, *Phys. Rev. Lett.* **30** (1973), 71-73.
- [59] Xavier Calmet, Basem Kamal El-Menoufi, Quantum Corrections to Schwarzschild Black Hole, *Eur. Phys. J. C* **77** (2017), 243.
- [60] Behnam Pourhassan, Salman Sajad Wani, Saheb Soroushfar, Mir Faizal, Quantum Work and Information Geometry of a Quantum Myers-Perry Black Hole, *JHEP* **10** (2021), 027, [arXiv:2102.03296].
- [61] Xavier Calmet, Folkert Kuipers, Quantum Gravitational Corrections to the Entropy of a Schwarzschild Black Hole, *Phys. Rev. D* **104** (2021), 066012.
- [62] Behnam Pourhassan, Izzet Sakalli, Non-perturbative correction to the Horava-Lifshitz black hole thermodynamics, *Chinese Journal of Physics* **79** (2022) 322-338, [arXiv:2210.07180].
- [63] Sudhaker Upadhyay, Nadeem ul Islam, Prince A. Ganai, A modified thermodynamics of rotating and charged BTZ black hole, *Journal of Holography Applications in Physics* **2** (2022), 25-48, [arXiv:1912.00767v2].
- [64] Ruben Campos Delgado, Quantum gravitational corrected evolution equations of charged black holes, *Journal of Holography Applications in Physics* **3** (2023), 39-48, [arXiv:2302.07835].
- [65] S. Garlip, Spacetime foam: a review, arXiv:2209.14282.

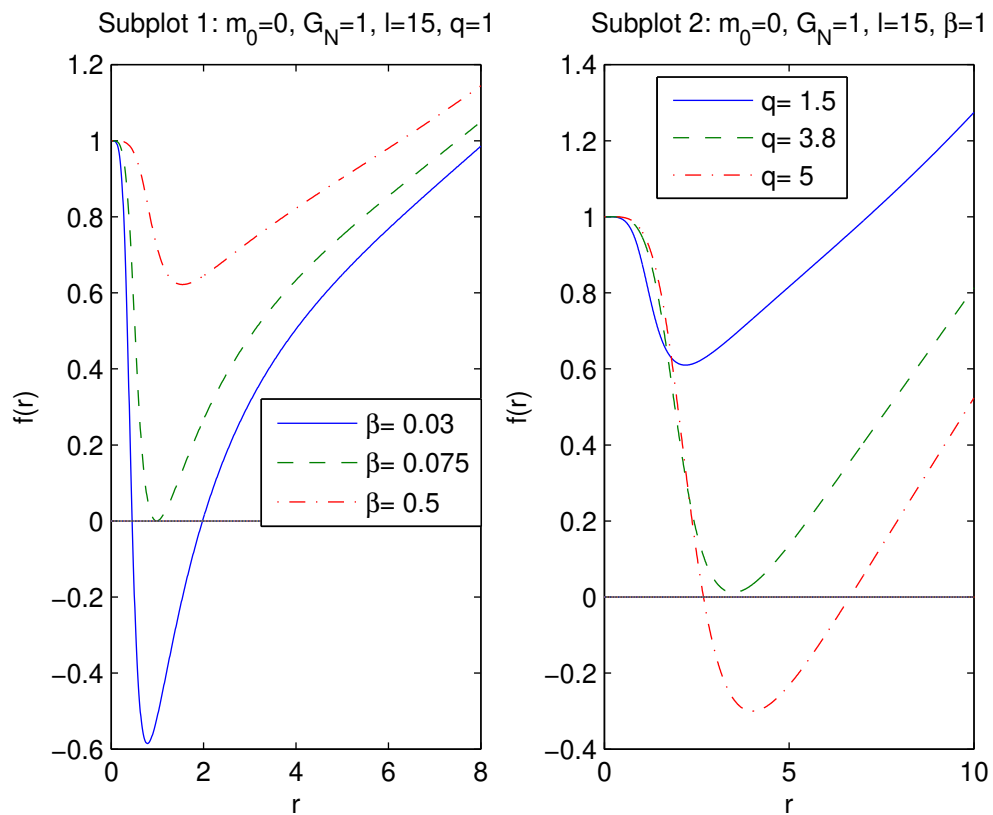


Figure 1: The metric function  $f(r)$  as a function of radius  $r$  at  $m_0 = 0$ ,  $G_N = 1$ ,  $l = 15$ . The left panel of Fig. 1 shows that when coupling  $\beta$  increases the event horizon radius decreases. In accordance with right panel of Fig. 1 if magnetic charge  $q$  increases the event horizon radius also increases.

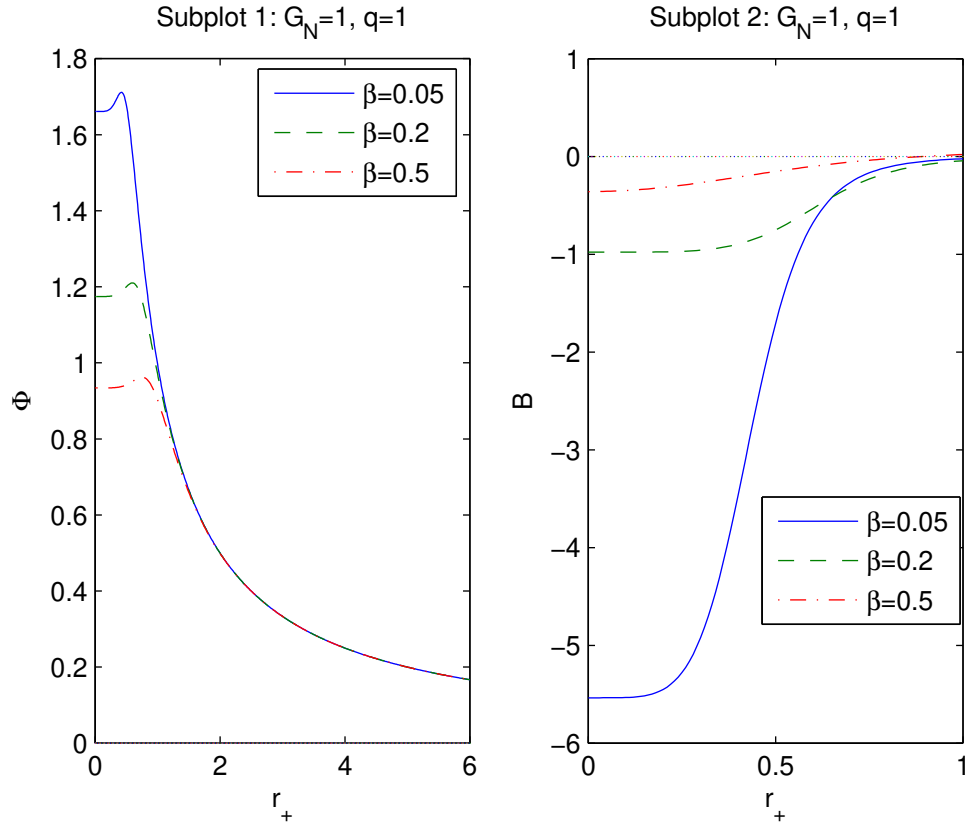


Figure 2: The functions  $\Phi$  and  $\mathcal{B}$  versus  $r_+$  at  $q = 1$ . The solid curve in the left panel corresponds to  $\beta = 0.05$ , the dashed curve is for  $\beta = 0.2$ , and the dashed-dotted curve corresponds to  $\beta = 0.5$ . One can see that the magnetic potential  $\Phi$  is finite at  $r_+ = 0$  and is zero as  $r_+ \rightarrow \infty$ . When NED parameter  $\beta$  increases the magnetic potential decreases. The function  $\mathcal{B}$  in the right panel becomes zero as  $r_+ \rightarrow \infty$  and is finite at  $r_+ = 0$ .

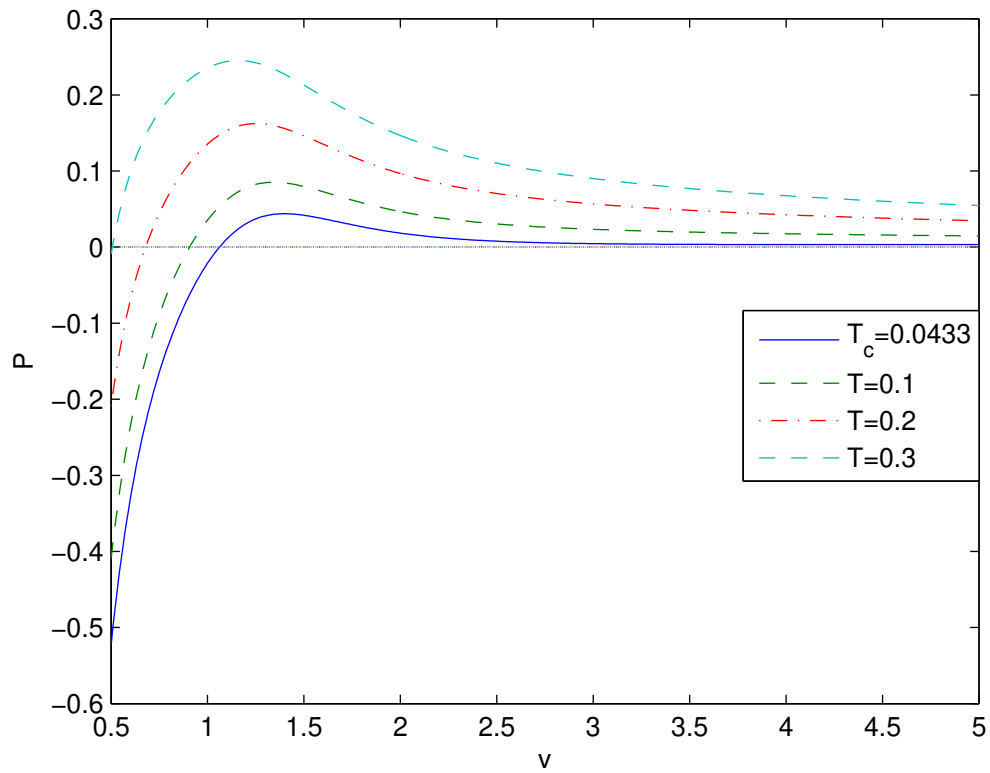


Figure 3: The function  $P(v)$  at  $q = 1$ ,  $\beta = 0.2$ . The critical isotherm corresponds to  $T_c \approx 0.0433$  having the inflection point.

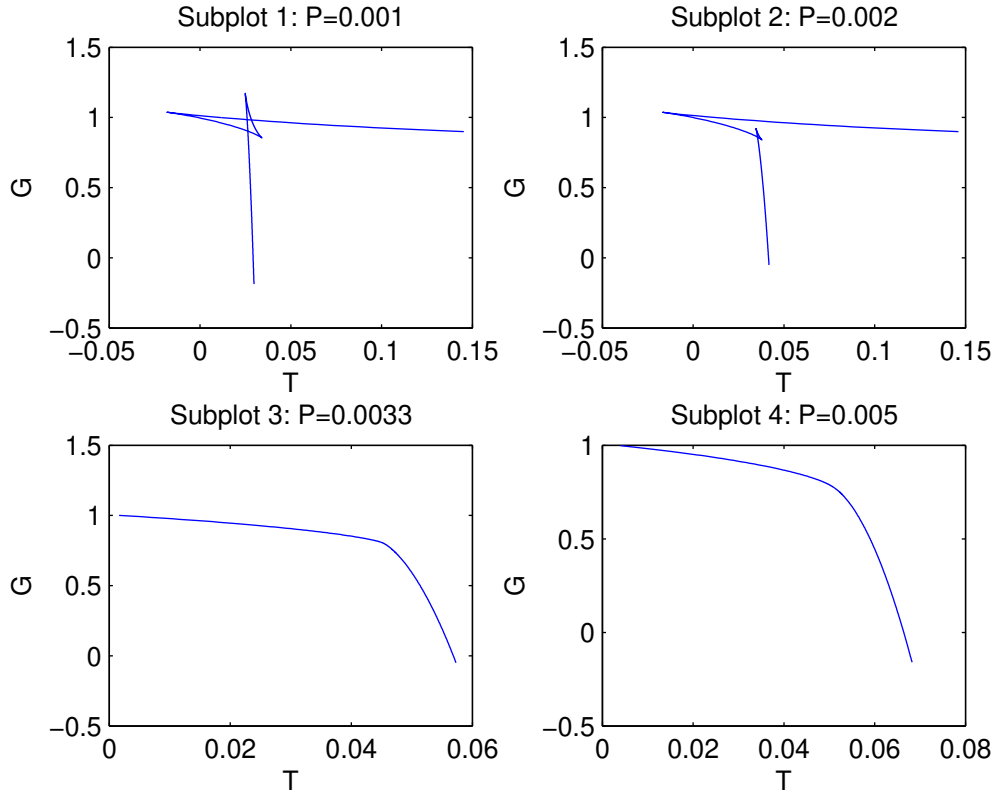


Figure 4: The plots of the Gibbs free energy  $G$  versus  $T$  at  $q = 1$ ,  $\beta = 0.2$ . Fig. 4 (subplots 1 and 2) shows 'swallowtail' plots resulting first-order phase transitions. Subplot 3 shows to second-order phase transition with  $P = P_c \approx 0.0033$ . Subplot 4 shows the case  $P > P_c$  with non-critical behavior of the Gibbs free energy.

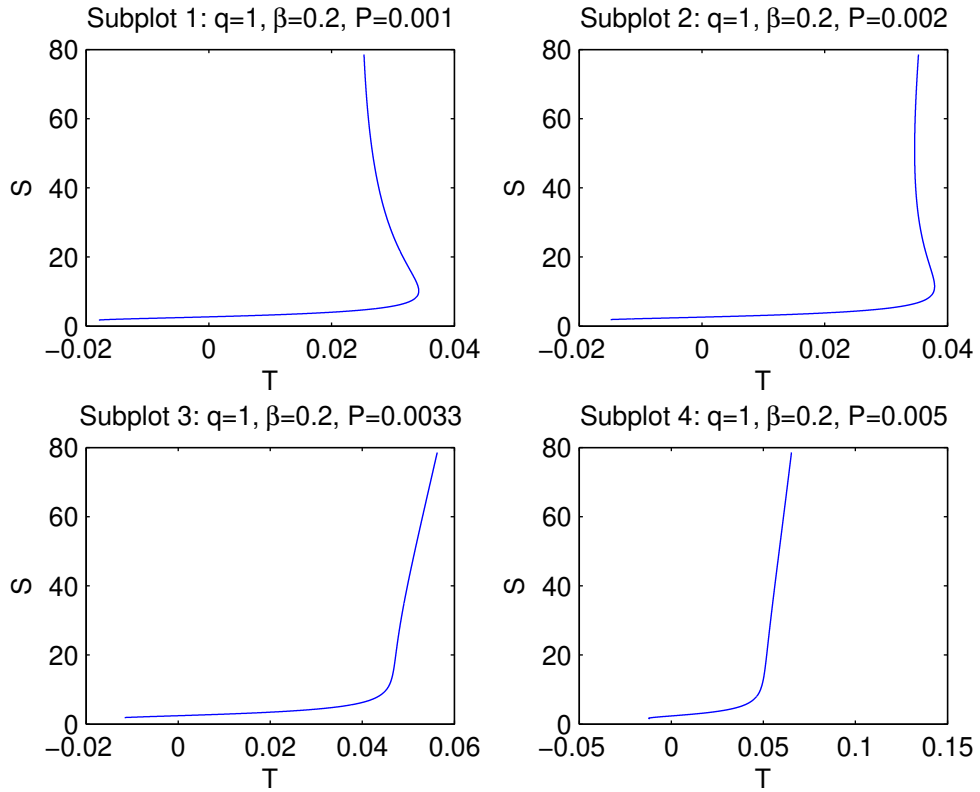


Figure 5: The plots of entropy  $S$  versus temperature  $T$  at  $q = 1$ ,  $\beta = 0.2$ . In accordance with subplots 1 and 2 entropy is ambiguous function of the temperature and, therefore, first-order phase transitions take place. According to subplot 3 the second-order phase transition occurs.

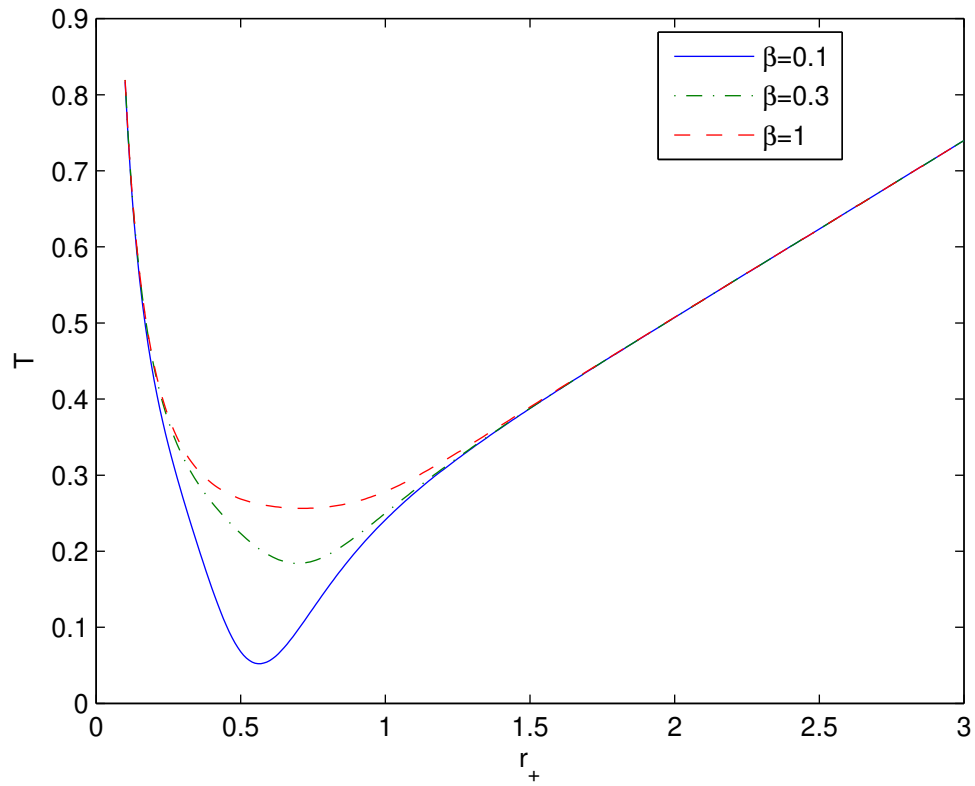


Figure 6: The plots of the Hawking temperature  $T$  versus horizon radius  $r_+$  at  $l = q = 1$ ,  $\beta = 0.1, 0.3, 1$ . In accordance with figures, the Hawking temperature possesses minima.



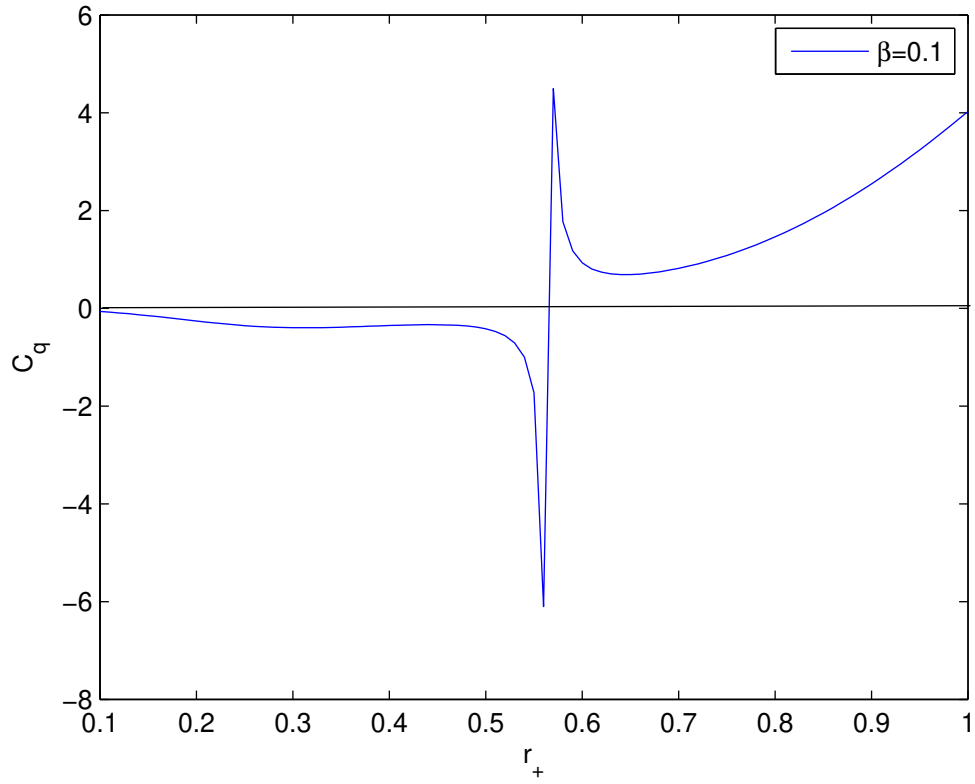


Figure 7: The plot of the heat capacity  $C_q$  versus horizon radius  $r_+$  at  $l = q = 1$ ,  $\beta = 0.1$ . According to the figure, the heat capacity has a singularity where the Hawking temperature possesses a minimum.

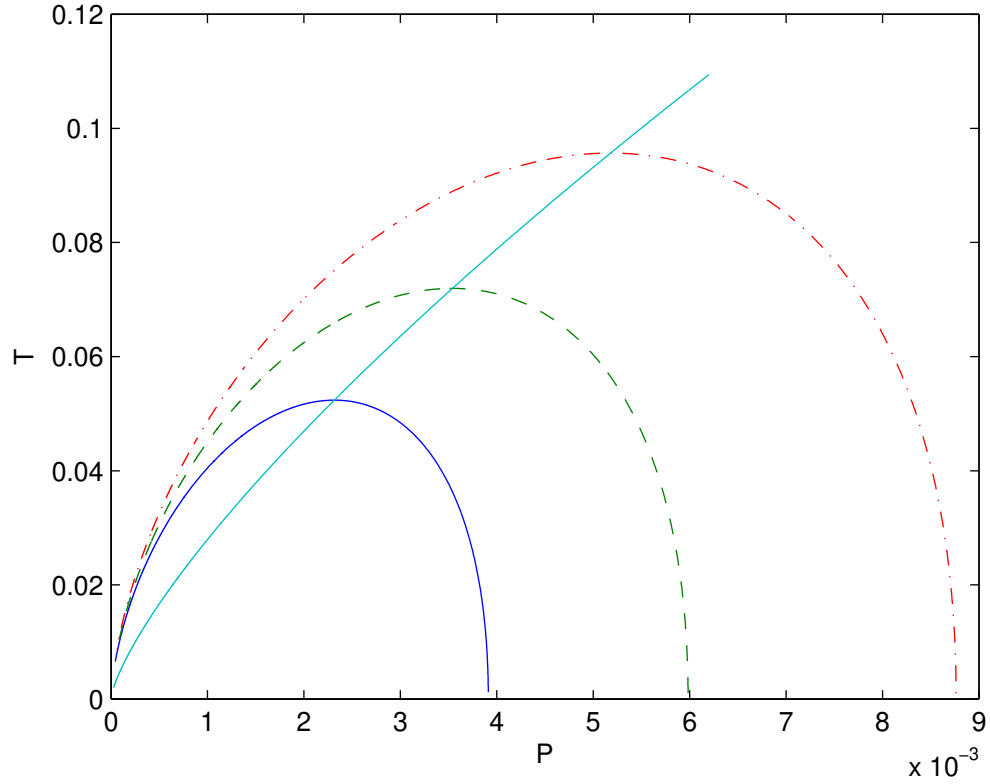


Figure 8: The plots of the temperature  $T$  versus pressure  $P$  at  $q = 40$ ,  $\beta = 0.2$ . The  $P_i - T_i$  diagram crosses maxima of isenthalpic curves. The solid curve corresponds to mass  $M = 100$ , the dashed curve is for  $M = 110$ , and the dashed-dotted curve corresponds to  $M = 120$ . When black hole masses increase the inversion temperature  $T_i$  also increases.

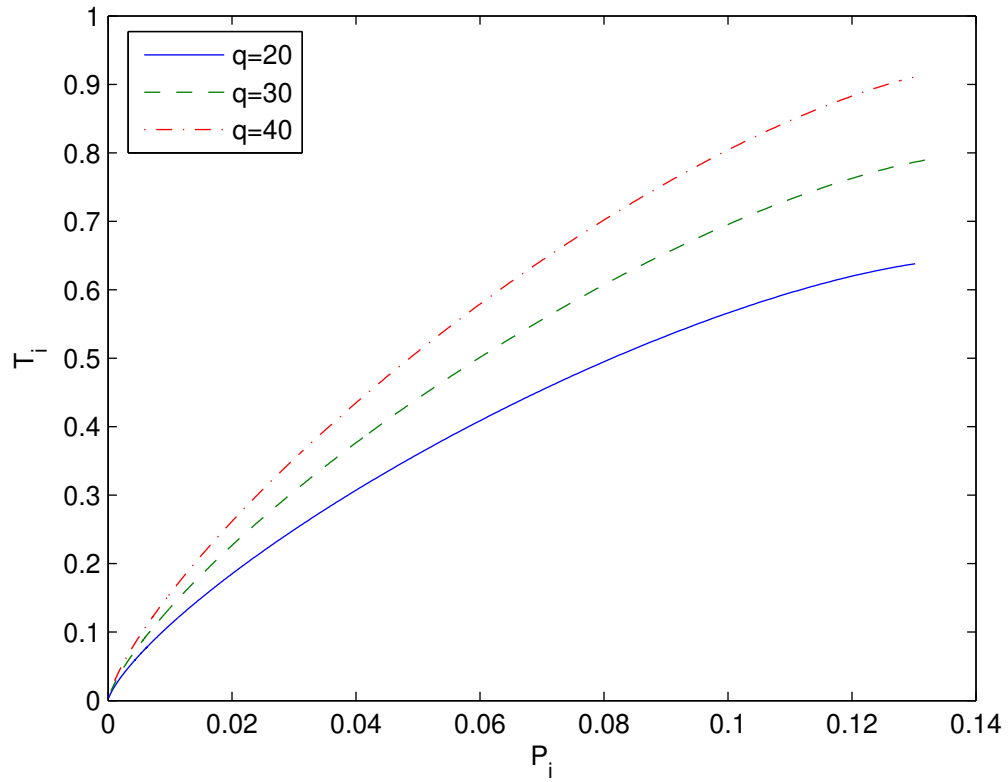


Figure 9: The inversion temperature  $T_i$  versus pressure  $P_i$  at  $q = 20, 30$  and  $40$ ,  $\beta = 0.2$ . When magnetic charge  $q$  increases the inversion temperature also increases.

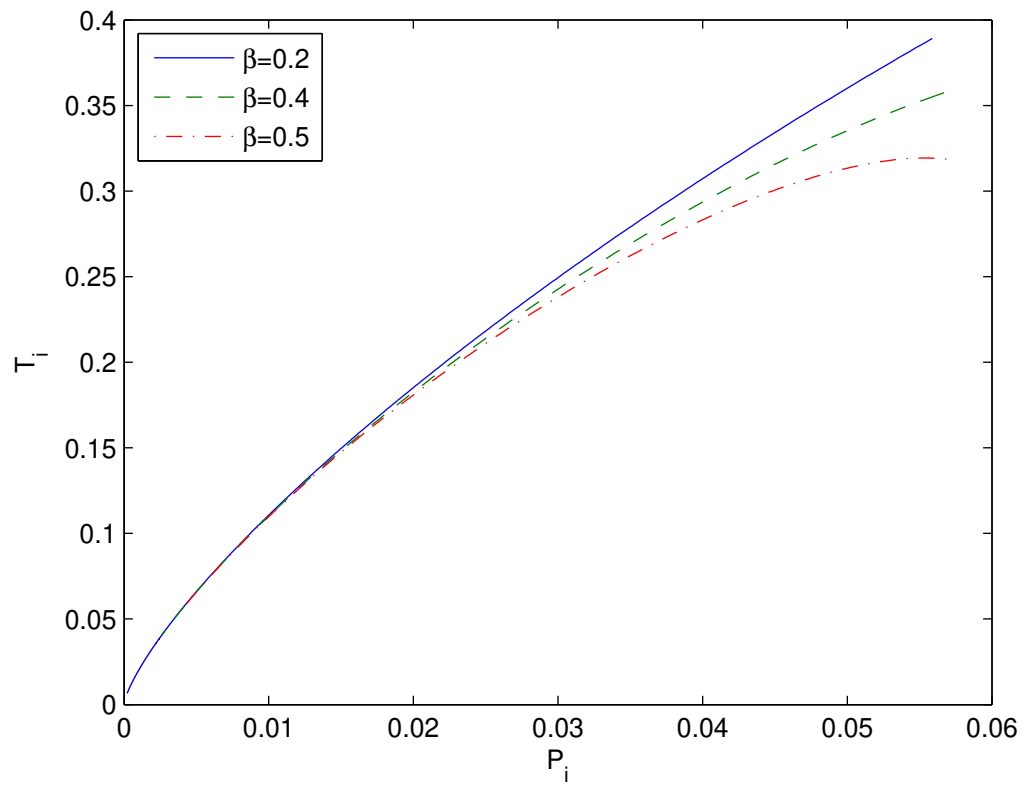


Figure 10: The inversion temperature  $T_i$  versus pressure  $P_i$  at  $\beta = 0.2, 0.4$  and  $0.5$ ,  $q = 20$ . When the coupling  $\beta$  increases the inversion temperature decreases.